RNA Biology 9:8, 1076-1087; August 2012; © 2012 Landes Bioscience

Loss of the abundant nuclear non-coding RNA *MALAT1* is compatible with life and development

Moritz Eißmann,[1,†] Tony Gutschner,[2,†] Monika Hämmerle,[2,3] Stefan Günther,[4] Maïwen Caudron-Herger,[5] Matthias Groß,[2] Peter Schirmacher,[3] Karsten Rippe,[5] Thomas Braun,[4] Martin Zörnig[1,*] and Sven Diederichs[2,*]

[1]Georg-Speyer-Haus; Frankfurt, Germany; [2]Helmholtz-University-Group "Molecular RNA Biology & Cancer"; German Cancer Research Center DKFZ & Institute of Pathology; University Hospital Heidelberg; Heidelberg, Germany; [3]Institute of Pathology; University Hospital Heidelberg; Heidelberg, Germany; [4]Max-Planck-Institute for Heart and Lung Research; Bad Nauheim, Germany; [5]Research Group Genome Organization & Function; German Cancer Research Center DKFZ & BioQuant; Heidelberg, Germany

[†]These authors contributed equally.

Keywords: long non-coding RNA, *MALAT1*, human knockout model, knockout mouse

Abbreviations: CLSM, confocal laser scanning microscopy; HCC, hepatocellular carcinoma; HP1, heterochromatin protein 1; KO, knockout; lncRNA, long non-coding RNA; *MALAT1*, *metastasis-associated lung adenocarcinoma transcript 1*; *NEAT1*, *nuclear enriched abundant transcript 1*; NSCLC, non-small cell lung cancer; Pc2: Polycomb 2 protein; qRT-PCR, quantitative reverse transcription-polymerase chain reaction; RNAP, RNA polymerase; RPLP0, ribosomal protein, large subunit, P0; TRF2, telomere repeat factor 2; UBF, upstream binding factor; WT, wild-type; ZFN, zinc finger nuclease

The *metastasis-associated lung adenocarcinoma transcript 1*, *MALAT1*, is a long non-coding RNA (lncRNA) that has been discovered as a marker for lung cancer metastasis. It is highly abundant, its expression is strongly regulated in many tumor entities including lung adenocarcinoma and hepatocellular carcinoma as well as physiological processes, and it is associated with many RNA binding proteins and highly conserved throughout evolution. The nuclear transcript *MALAT-1* has been functionally associated with gene regulation and alternative splicing and its regulation has been shown to impact proliferation, apoptosis, migration and invasion.

Here, we have developed a human and a mouse knockout system to study the loss-of-function phenotypes of this important ncRNA. In human tumor cells, *MALAT1* expression was abrogated using Zinc Finger Nucleases. Unexpectedly, the quantitative loss of *MALAT1* did neither affect proliferation nor cell cycle progression nor nuclear architecture in human lung or liver cancer cells. Moreover, genetic loss of *Malat1* in a knockout mouse model did not give rise to any obvious phenotype or histological abnormalities in *Malat1*-null compared with wild-type animals. Thus, loss of the abundant nuclear long ncRNA *MALAT1* is compatible with cell viability and normal development.

Introduction

Recent deep transcriptome sequencing and tiling array studies have uncovered that between 70% and 90% of the human genome are estimated to be pervasively transcribed into mostly non-protein-coding RNA while only less than 2% of the human genome are encoding for proteins.[1-4] These non-coding RNAs (ncRNAs) comprise small RNAs such as microRNAs[5] as well as long non-coding RNAs (lncRNAs). However, only a minute fraction of the large number of non-coding gene products has been identified or characterized at all. The few individual examples studied in greater detail provide evidence that lncRNAs can execute a broad range of important functions in the cell.[6-8] Individual long ncRNAs have been implicated e.g., in gene regulation,[9-11] splicing control,[12-14] or X chromosome dosage compensation.[15,16] Notably, some of the lncRNAs have also been implicated in human diseases and most importantly in cancer where lncRNAs can be deregulated or actively contributing to tumorigenesis.[17-20]

One of the first lncRNA genes discovered was *MALAT1*, the *metastasis-associated lung adenocarcinoma transcript 1*,[21] later also referred to as *NEAT2* for *nuclear-enriched abundant transcript 2*. *MALAT1* is highly abundant and is expressed in many healthy organs, most strongly in pancreas and lung.[21] Deregulation or a functional role for *MALAT1* have now been established in many human cancer entities including lung cancer, hepatocellular carcinoma (HCC), uterine endometrial stromal sarcoma, cervical cancer, breast cancer, osteosarcoma and colorectal cancer, but *MALAT1* has also been linked to viral infection or alcohol abuse.[21-29] In non-small cell lung cancer (NSCLC), *MALAT1* is significantly associated with metastasis and serves as an independent prognostic marker for patient survival in early stage lung adenocarcinoma or squamous cell carcinoma of the lung.[21,30] It promotes cell motility of lung cancer cells[31] and supports

*Correspondence to: Martin Zörnig and Sven Diederichs; Email: zoernig@em.uni-frankfurt.de and s.diederichs@dkfz.de
Submitted: 06/04/12; Accepted: 06/11/12
http://dx.doi.org/10.4161/rna.21089

proliferation and invasion of cervical cancer cells by regulating CASPASE-8, CASPASE-3, BAX, BCL-2 and BCL-XL.[22] Furthermore, *MALAT1* is functionally important for trophoblast invasion during embryonic development[32] and is associated with synaptogenesis.[33] In summary, *MALAT1* is strongly expressed in many tissues, significantly regulated under various physiological and pathological conditions and has been linked to a plethora of functions at the cellular level including proliferation, apoptosis, migration or invasion.

At the molecular level, multiple functions have been proposed for *MALAT1*.[11,13,14,33,34] *MALAT1* is retained in the nucleus and specifically localizes to nuclear SC35 speckles that play a role in pre-mRNA processing.[35] *MALAT1* might regulate alternative pre-mRNA splicing by modulating the phosphorylation levels of serine/arginine splicing factors.[13] Depletion of *MALAT1* might alter the pre-mRNA processing of tissue factor or endoglin transcripts.[34] Importantly, *MALAT1* might interact with the polycomb repressive complex 1 (PRC1) and thus controls the relocation of growth control genes between polycomb bodies and interchromatin granules, places of silent or active gene expression, respectively.[11] Additionally, *MALAT1* RNA is frequently found in many PAR-CLIP experiments as a common interaction partner of RNA binding proteins potentially indicating further functions of *MALAT1*.[36,37] Also, the *MALAT1* transcript can be processed into a tRNA-like small cytoplasmic RNA, the mascRNA, which might fulfill additional, so far unknown functions.[38] Given all of these divergent potential activities, *MALAT1* could function in a cell type- or tissue-specific manner despite its ubiquitous expression. Finally, *MALAT1* is highly conserved throughout evolution across many mammalian species, underscoring its potential functional importance (**Fig. 1A**).

In summary, these various lines of evidence culminate in the hypothesis that *MALAT1* must be an important and most likely essential gene given its high and ubiquitous abundance, its specific regulation and localization patterns, its evolutionary conservation, its many interaction partners, molecular mechanisms and the strong impact of its deregulation on many cellular phenotypes including fundamental processes such as proliferation, migration or invasion.

The functional characterization of lncRNAs has greatly been hampered by a lack of quantitative loss-of-function models. Many lncRNAs–especially if they are nuclear, highly abundant or highly structured–can only be ineffectively targeted by RNA interference. In particular, this is a concern for studies of the highly abundant *MALAT1*, which was reduced only two- to 4-fold by shRNAs or siRNAs.[30,31] Accordingly, these approaches make it difficult to distinguish between specific and off-target effects and their results may be prone to false-negative results due to an insufficient knockdown. Genetic knockout models have only been established for very few lncRNAs. For example, the *Malat1*-neighboring lncRNA *Neat1 (nuclear enriched abundant transcript 1)*, which is essential for paraspeckle formation, has been knocked out in mice, but no phenotype has been reported so far.[39,40] To overcome this challenge and to create quantitative loss-of-functions models, we have developed a strategy to generate functional lncRNA knockouts also in human cell lines using zinc finger nucleases to stably integrate RNA destabilizing elements into the human genome site-specifically at the start of an lncRNA gene.[41]

Here, we exploit this technique and achieve the efficient silencing of *MALAT1* expression in human lung and liver cancer cells. Surprisingly, we demonstrate that the lncRNA *MALAT1* is not essential for cell proliferation, cell cycle progression or maintenance of nuclear architecture. Our human loss-of-function model is complemented by a *Malat1* knockout mouse model. *Malat1*-null mice are viable and without any histological signs of developmental defects. Thus, the loss of the highly abundant, nuclear enriched and evolutionarily conserved lncRNA *MALAT1* is unexpectedly compatible with life and development.

Results

Depletion of *MALAT1*, a highly conserved and abundant lncRNA, from human cancer cells. As a first indication for the putative functional relevance of *MALAT1*, we verified its evolutionary conservation, strong expression and regulation. The lncRNA *MALAT1* displayed a high level of sequence conservation throughout 33 mammalian species (**Fig. 1A**). In human cells, *MALAT1* showed a ubiquitous expression, as it is detected in immortalized primary human cells (1°FF and HEK293) as well as in a broad range of cancer cell lines derived from different tissues (**Fig. 1B**, left panel). In addition, *MALAT1* was highly abundant and even exceeded the expression of classical housekeeping genes like for example RPLP0 (ribosomal protein, large, P0) (**Fig. 1B** right panel).

Based on this pattern of conservation and high expression, we aimed for unraveling the role of *MALAT1* in cancer cells as well as in normal development. Therefore, we employed an innovative approach that we recently developed to create highly specific and efficient loss-of-function models of abundant ncRNAs in human cancer cell lines.[41] This approach relies on the stable and site-specific integration of RNA destabilizing elements into the cancer cell genome mediated by zinc finger nucleases (ZFNs) (**Fig. 1C**). The ZFN binds to a specific site in the genome and introduces a DNA doublestrand break. When a repair template is present, this break is repaired via homologous recombination allowing a site-specific integration of exogenous sequences. Here, we integrate a cassette comprising the green fluorescent protein (GFP) as a selection marker and a polyadenylation signal (polyA), which functions as the RNA destabilizing element silencing downstream sequences.

Previously, we had only generated A549 bulks of lung adenocarcinoma cells deficient of *MALAT1*.[41] Here, we extended the loss-of-function model to the liver cancer line HLE (hepatocellular carcinoma). As in A549 cells, *MALAT1* was specifically and very efficiently suppressed in stable HLE lines. We obtained single cell *MALAT1* knockout clones (KO) in both cancer cell lines with a 1000-fold reduction of *MALAT1* expression in A549 KO clones and over 200-fold reduction of *MALAT1* in HLE KO clones (**Fig. 1D**). This approach depleted the full-length *MALAT1* transcript: two different qRT-PCR primer pairs located at either

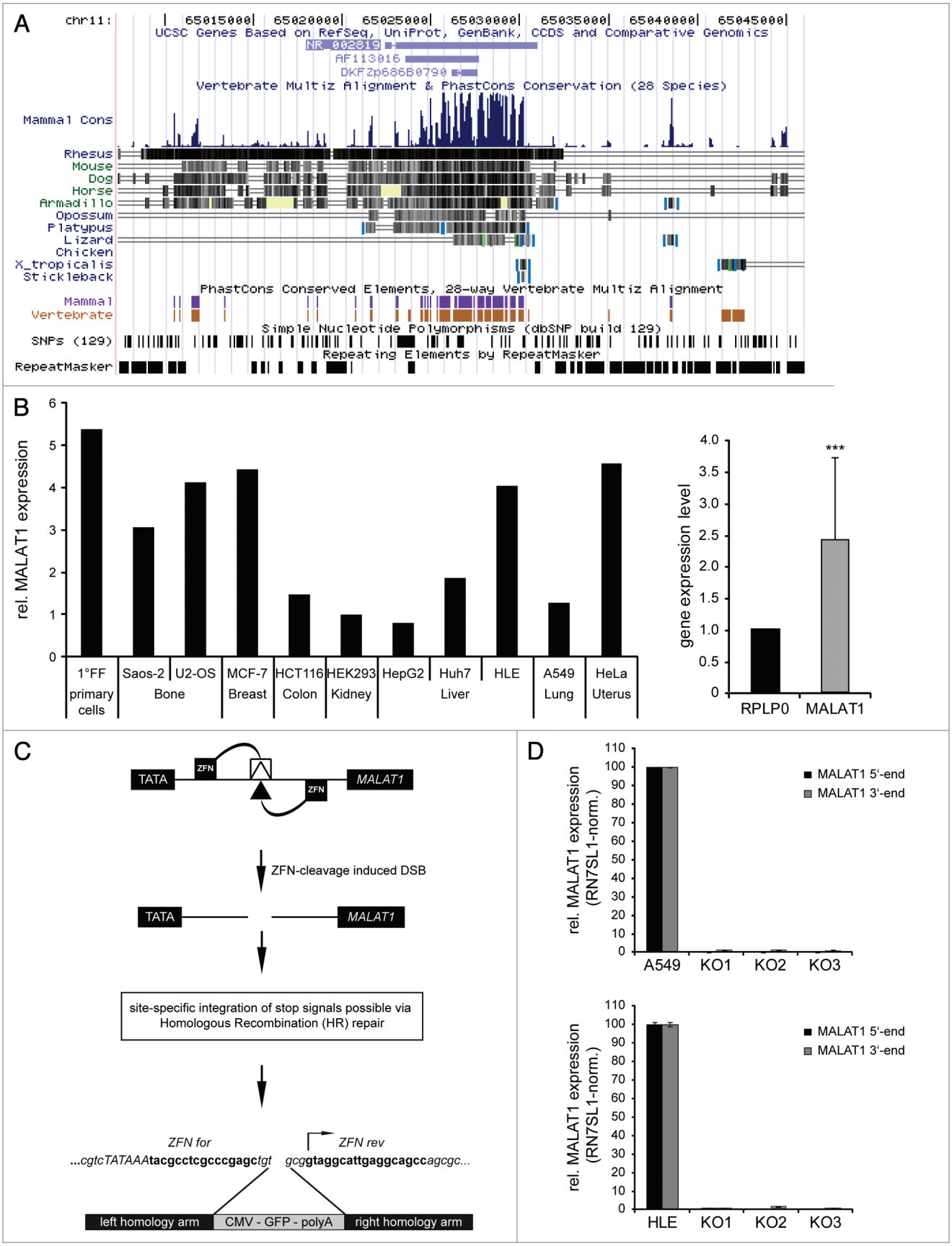

Figure 1. See figure legend on p. 1079.

Figure 1. (see previous page) Expression and depletion of *MALAT1* in human cells. (A) The evolutionary conservation of *MALAT1* over its entire length is depicted using the University of California, Santa Cruz (UCSC) genome browser. (B) *MALAT1* expression was determined in a panel of 11 human cell lines representing different tissues of origin. Shown is the expression relative to RPLP0 mRNA (B, left panel). On average, *MALAT1* shows a 2.5-fold higher expression ($p < 0.001$) in these cell lines compared with the abundant housekeeping gene RPLP0 (B, right panel). (C) To deplete the highly abundant lncRNA *MALAT1*, a knockout approach was recently developed[41] that is schematically explained here. (D) This method allowed the generation of A549 (lung) and HLE (liver) single cell clones that showed a ~1000-fold or ~200-fold reduction of full-length *MALAT1*, respectively. Given is the average expression measured in three independent experiments +SEM.

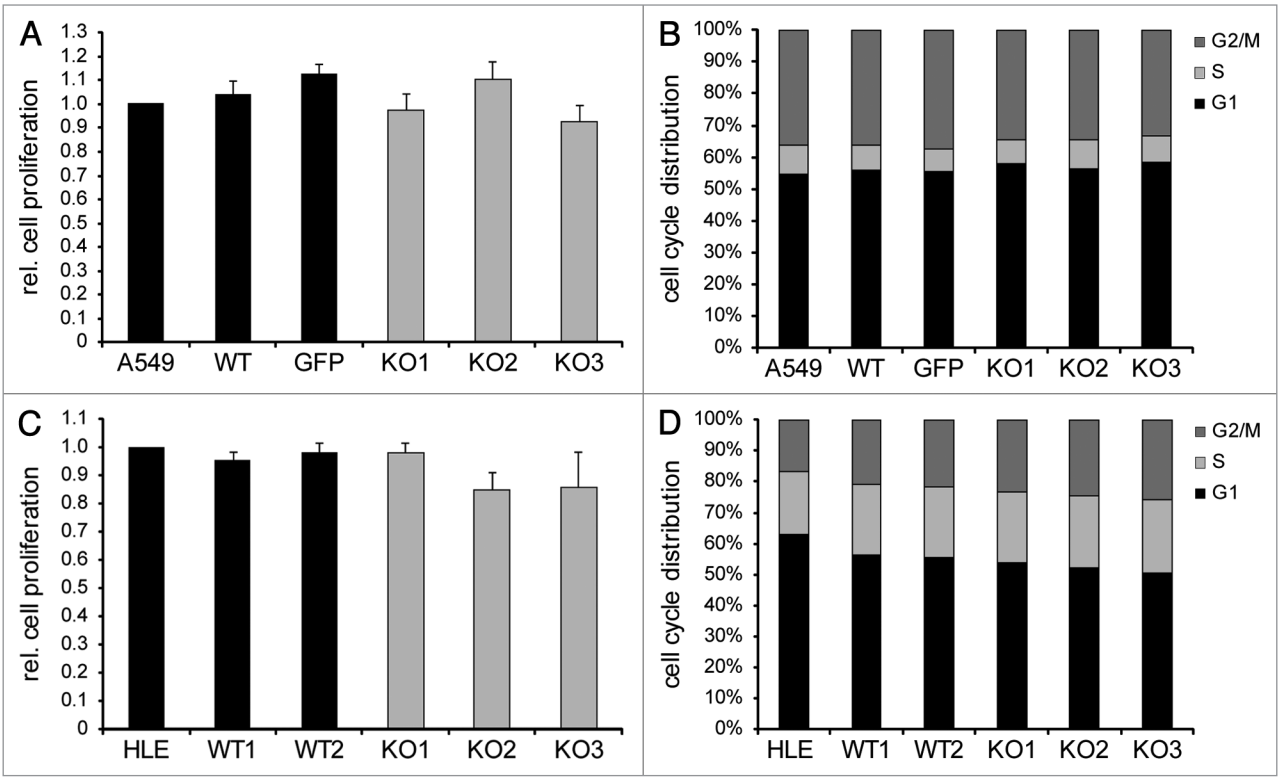

Figure 2. Proliferation and cell cycle progression of *MALAT1* KO cells. The proliferative phenotype of A549 and HLE *MALAT1* WT and KO cells was analyzed. (A+C) For both cell lines, relative proliferation rates were determined using a bromodeoxyuridine (BrdU) proliferation assay. Results were normalized to the parental cell line in each case. Mean values of three independent experiments +SEM are presented. (B+D) Cell cycle profiles were obtained from exponentially growing cells and the average percentages of cells in G1-, S- and G2/M-phase from at least two independent experiments are depicted.

end of the *MALAT1* transcript yielded the same negative results for *MALAT1* expression in the knockout cell clones (**Fig. 1D**).

***MALAT1* is not critical for lung or liver cancer cell proliferation.** One of the most prominent characteristics of cancer cells is their ability to proliferate–even in the absence of external stimuli due to deregulated signaling cascades. We used our knockout system to analyze the role of *MALAT1* in lung and liver cancer cell proliferation. Therefore, we performed cell cycle analyses and proliferation assays with a panel of three *MALAT1* wild-type (WT) control cell lines and three KO clones per cell line (**Fig. 2A-D**). As control cells, we included the parental cell lines (A549; HLE) and two WT single cell clones for each cell line that had undergone clonal selection at the same time as the KO clones. We compared the proliferation between WT and KO clones, but could not detect any significant differences in bromodeoxyuridine assays (**Fig. 2A and C**). Additionally, the cell cycle profiles did not significantly differ between WT and KO clones with similar fractions of cells in G1-, S- and G2/M-phase, respectively (**Fig. 2B and D**). Thus, complete loss of *MALAT1* did not impact cell proliferation or cell cycle progression in the lung and liver cancer cells studied here.

Loss of *MALAT1* does not affect the global nuclear architecture. A number of studies point to a crucial role of RNA as an architectural factor for shaping the genome and its nuclear environment.[42] Since *MALAT1* is a highly abundant RNA strongly enriched in the nucleus, we hypothesized that its loss might affect the structural organization of the nucleus.[35,38] Accordingly, we examined the effect of the *MALAT1* knockout with respect to several nuclear subcompartments for which an architectural role of RNA has been reported previously. RNA-dependent changes in nuclear morphology at a resolution of 200–300 nm can be directly detected after fluorescent labeling via evaluation of optical sections acquired by confocal laser scanning microscopy (CLSM) as demonstrated in RNase microinjection experiments.[43]

In the latter study, a compaction of the DNA distribution after DAPI staining revealed that nuclear RNAs are needed to maintain transcriptionally active chromatin compartments in a decondensed conformation. Active RNA polymerase II (RNAP II) can be visualized with an appropriate antibody and associates into distinct nuclear foci referred to as "transcription factories."[44] Accordingly, we tested whether the knockout of *MALAT1* resulted in changes of the nuclear distribution of chromatin (DAPI, blue color in merged images in **Fig. 3**), RNA (5-ethynyl-uridine label, **Fig. 3A**) and RNAP II transcription factories (immunofluorescence, **Fig. 3B**). No effect of the *MALAT1* knockdown was apparent. In addition, the formation of additional lamin A invaginations in murine cells have been reported upon RNase A treatment.[43] In *MALAT1* KO cells, the nuclear envelope structure did not change according to the lamin A staining (**Fig. 3C**).

The nucleolus is a site of active RNAP I transcription and is also known to be dependent on RNAP II transcription since its inhibition results in the dissolution of nucleoli into so-called "necklace" structures.[42] The abundant *MALAT1* transcript is found as an RNA component in purified nucleoli (Caudron-Herger and Rippe, unpublished), and we reasoned that *MALAT1* could play a role for maintaining the structural integrity of the nucleolus. This was tested with UBF (upstream binding factor) as a marker protein for active rDNA genes. UBF reorganizes in the nucleus when the nucleolus structure is disrupted by RNAP II inhibition with α-amanitin. However, no differences were observed here between wild-type and *MALAT1* knockout cells (**Fig. 3D**).

MALAT1 had previously been closely linked to SC35 nuclear domains,[35] that are also referred to as splicing/nuclear speckles or interchromatin granules. RNA is an important structural component of these nuclear subcompartments.[45,46] Unmethylated Pc2 (Polycomb 2) protein binds to *MALAT1* in SC35 domains and thereby relocates growth-control genes to a nuclear environment that promotes their expression.[11] The knockdown of *MALAT1* by RNA interference resulted in a redistribution of growth-control gene promoters between PcG bodies and SC35 domains toward the silencing environment of PcG bodies.[11] Thus, another potential function of *MALAT1* could be maintaining the structure of SC35 domains and / or mediating interactions of genes with this nuclear subcompartment. However, within the resolution provided by our CLSM analysis, wild-type and knockout cells displayed no significant structural differences with respect to SC35 immunofluorescence (**Fig. 3E**). Upon close inspection of confocal three dimensional stacks, it appeared that in some knockout cells the borders of the SC35 domains were slightly more diffuse than in wild-type cells. However, due to the irregular structure of the splicing speckles, we were unable to confirm the statistical significance of this observation.

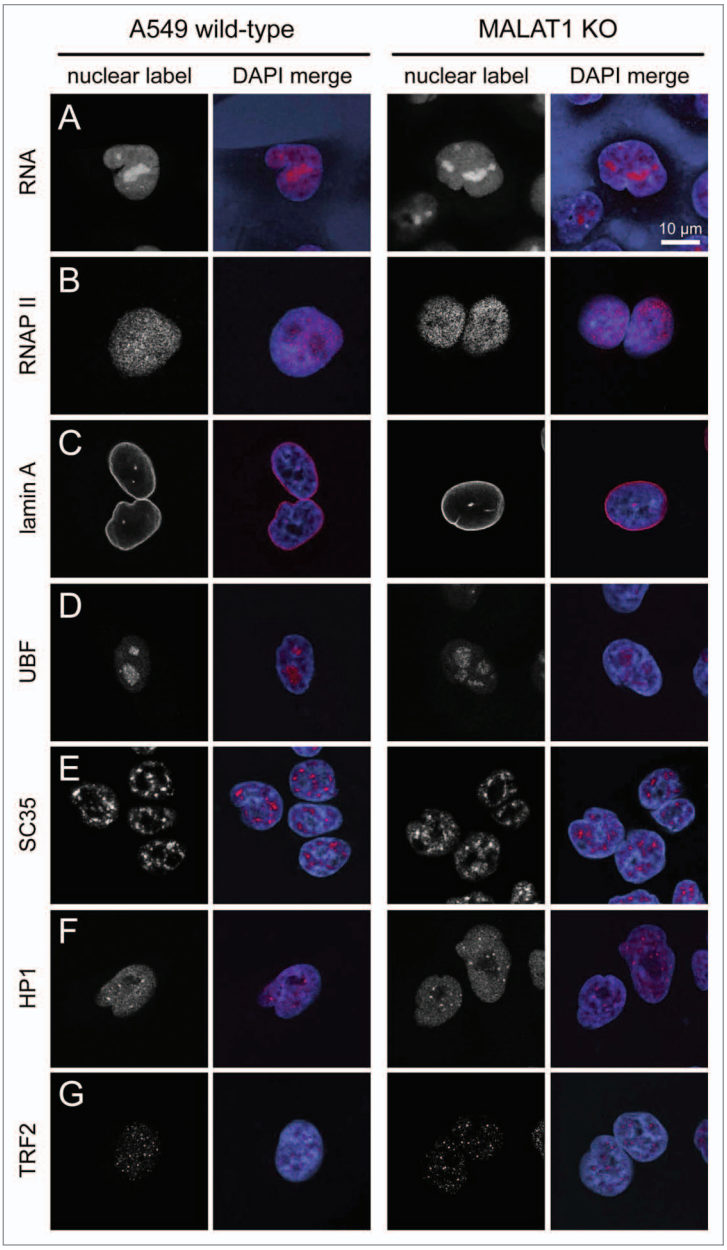

Figure 3. Nuclear morphology of human A549 wild-type and *MALAT1* knockout cells. CLSM optical sections were acquired for different fluorescently labeled nuclear components in the A549 lung cancer cell line for wild-type and *MALAT1* knockout cells. RNA was labeled via incorporated 5-ethynyl-uridine, and the proteins were visualized by immunofluorescence. The merged images show the indicated nuclear components in red and a DNA DAPI staining in blue. Scale bar, 10 μm. (A) RNA labeled. (B) Active RNA polymerase II. (C) Lamin A, a component of the nuclear envelope. (D) UBF, a marker for active ribosomal genes. (E) Splicing speckles visualized via the SC35 protein. (F) HP1α, enriched in pericentric heterochromatin. (G) TRF2, localizing to the telomeric shelterin complex.

As discussed previously, a number of proteins that fulfill architectural functions for the formation of heterochromatic regions at the pericentromeres, centromeres and telomeres are targeted to these chromosomal loci via RNA.[42] Accordingly, we investigated heterochromatin protein 1 α (HP1α) as a factor involved in establishing and maintaining the repressive state of pericentric heterochromatin and telomere repeat factor 2 (TRF2) as a marker

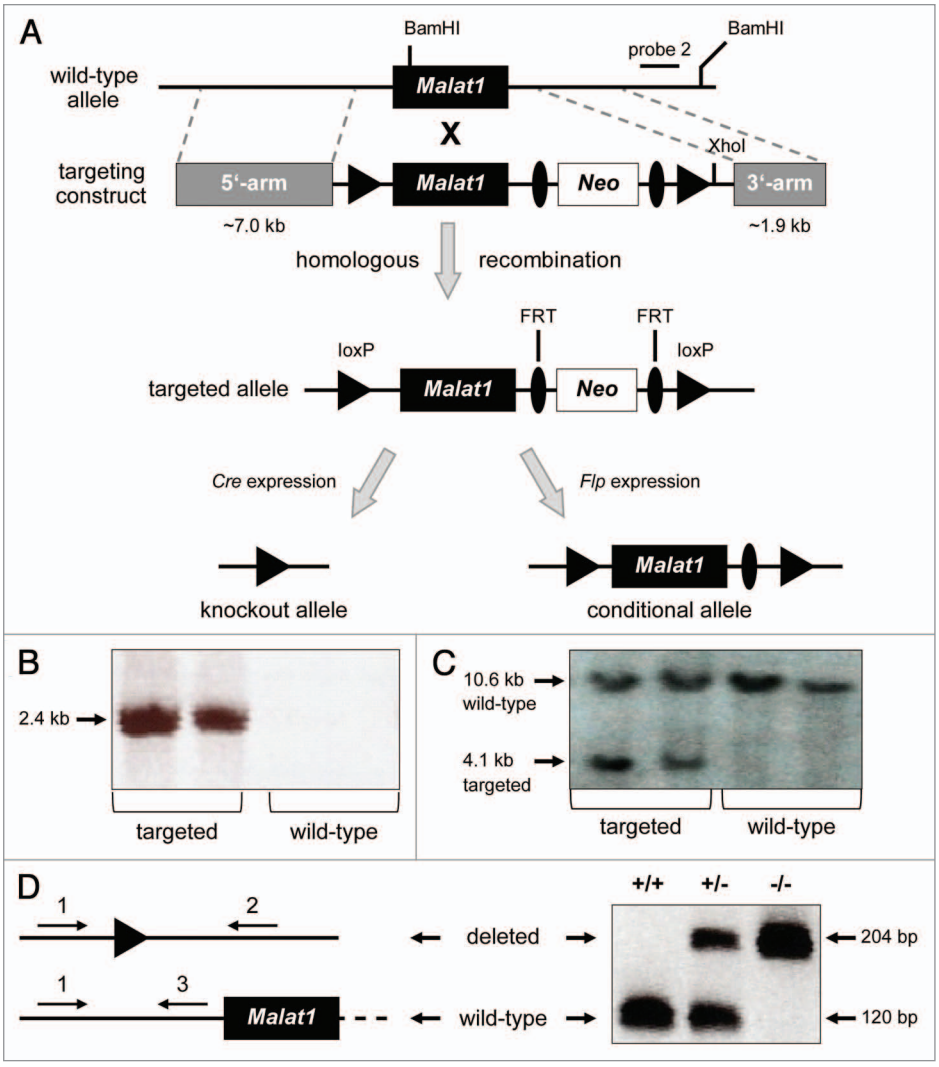

Figure 4. Generation and confirmation of the *Malat1* knockout mouse line. (A) Schematic presentation of the strategy for deletion of *Malat1* by homologous recombination in the mouse genome. LoxP (Cre recombination) and FRT (Flip recombination) sites are indicated and allow individual removal of the complete *Malat1* locus (Cre) and the Neomycin (neo) resistance gene (Flip), respectively. Probe 2: 3'external probe (located outside of the targeting vector) for Southern blot analysis. (B) PCR analysis of genomic DNA prepared from single electroporated ES cell clones. With the forward primer located in the neo resistance gene and the reverse primer hybridizing to the wild-type sequence at the 3'-end outside of the targeting construct, several ES cell clones with the desired homozygous recombination were identified via a 2420 bp PCR fragment which is absent in clones without correct targeting. (C) Southern Blot analysis with genomic DNA prepared from single electroporated ES cell clones and digested with the restriction enzymes BamHI and XhoI. Probe 2 recognized a 4.1 kb XhoI/BamHI fragment in the correctly targeted locus, while the wild-type allele was identified via a 10.6 kb BamHI/BamHI fragment. All relevant restriction sites are indicated in (A). (D) To confirm Cre-mediated deletion of *Malat1* and to distinguish wild-type, heterozygous and homozygous *Malat1* constitutive knockout mice, a three-primer-PCR-strategy was developed, resulting in two fragments with different lengths for the wild-type (120 bp) and the targeted (204 bp) locus.

for the telomere shelterin complex. For both proteins, no changes in the nuclear localization were observed in the *MALAT1* knockout as compared with the wild-type cell line (**Fig. 3F and G**). Thus, loss of *MALAT1* had no detectable impact on the nuclear structures analyzed here.

Generation and analysis of *Malat1*-deficient knockout mice. To investigate the physiological function of *Malat1* and to study the consequences of *Malat1* deficiency in vivo, we established an inducible *Malat1* knockout mouse model by homologous recombination in murine embryonic stem (ES) cells. The complete 6,982 bp long *Malat1* sequence was deleted, including 250 nucleotides upstream of the transcriptional start site and 321 nucleotides following the 3'-end of the *Malat1* transcript. Detailed information on the production of the knockout mice is provided in the Materials and Methods section. A schematic presentation of the targeted *Malat1* locus, its construction by homologous recombination in ES cells as well as Cre- and Flp-mediated deletions in mice are shown in **Figure 4A**. Verification of correct *Malat1* targeting in ES cells and mice were performed by PCR and Southern Blot analysis (**Fig. 4B and C**).

For our initial analysis, we generated mice with a constitutive knockout of *Malat1* by mating of animals harboring one conditional knockout allele with transgenic CMV-Cre deleter mice. The Cre-mediated deletion of *Malat1* was confirmed by PCR analysis (**Fig. 4D**).[47] The resulting heterozygous knockout mice were bred with each other to obtain *Malat1*-deficient offspring. Surprisingly, homozygous *Malat1*$^{-/-}$ mice were born alive, without indication of embryonic lethality (in total, 15 homozygous *Malat1*$^{-/-}$ knockout mice, 21 heterozygous *Malat1*$^{+/-}$ knockout animals and 7 wild-type *Malat1*$^{+/+}$ mice were obtained), and these animals displayed no apparent phenotype or pathological limitations when kept under normal stress-free conditions.

***Malat1* and *Neat1* expression after knockout of *Malat1*.** To validate the effective knockout of *Malat1* in the mouse model, we determined the expression of *Malat1* transcripts in eight different organs by qRT-PCR (**Fig. 5A**). As expected, *Malat1* expression was absent in all tissues obtained from homozygous *Malat1* knockout mice. Importantly, we used three different amplicons covering the entire length of *Malat1* to validate the quantitative loss of *Malat1* over the entire transcript. Additionally, the expression of the lncRNA *Neat1* was determined using two independent amplicons. *Neat1* is a nuclear lncRNA that is essential for paraspeckle formation[39] and represents the neighboring transcript

upstream of *Malat1*. In only four out of eight organs, we detected a slight, but non-significant induction of *Neat1* in *Malat1*-negative tissues arguing against a hypothetical role of *Malat1* in regulating *Neat1* expression *in cis*.

In the human *MALAT1*-deficient cell lines, *NEAT1* expression also remained unaltered (**Fig. 5B**).

Histomorphological analysis of WT and *Malat1* KO organs. Different organs of *Malat1* KO mice were analyzed histomorphologically, including brain, heart, lung, thymus, liver, spleen, pancreas, kidney, intestine and genitals (ovary and testis). Notably, we did not observe any differences related to organ development, organ architecture or organ size. Moreover, no tumors or signs of inflammation were detected in any of the analyzed tissues. Representative pictures of two wild-type (♀, ♂; **Fig. 6**, left panel) and two knockout mice (♀, ♂; **Fig. 6**, right panel) of brain, thymus, lung, liver, pancreas, kidney and genitals are shown.

Brain sections show proper assembly of the brain cortex with pyramidal neurons and oligodendroglial cells (**Fig. 6A**). Thymic parenchyma is regularly divided into a cortical portion with densely packed lymphoid cells and a pale stained medullary portion (**Fig. 6B**). Lung tissue showed a regular alveolar structure both in WT and *Malat1* KO mice without any signs of edema, congestion or emphysema (**Fig. 6C**). Liver parenchyma displayed the characteristic lobular organization with hexagonal appearance based on the distributions of portal areas and central venules. No signs of fibrosis or inflammation were visible (**Fig. 6D**). Pancreatic tissue of both wild-type and *Malat1* knockout mice was regularly subdivided into the exocrine part composed of acini and the pale stained endocrine part with prominent islets of Langerhans (**Fig. 6E**). Mouse kidneys of WT and *Malat1* KO mice showed a regular assembly of renal cortex showing glomeruli and tubules (**Fig. 6F**) as well as regularly structured medulla with loops of Henle and collecting ducts. Neither female nor male genitals, namely ovary and testis, showed any signs of developmental defects or false organ assembly showing characteristic ovarian follicles and tubular appearance of the testes (**Fig. 6G**). Thus, the viable *Malat1* KO

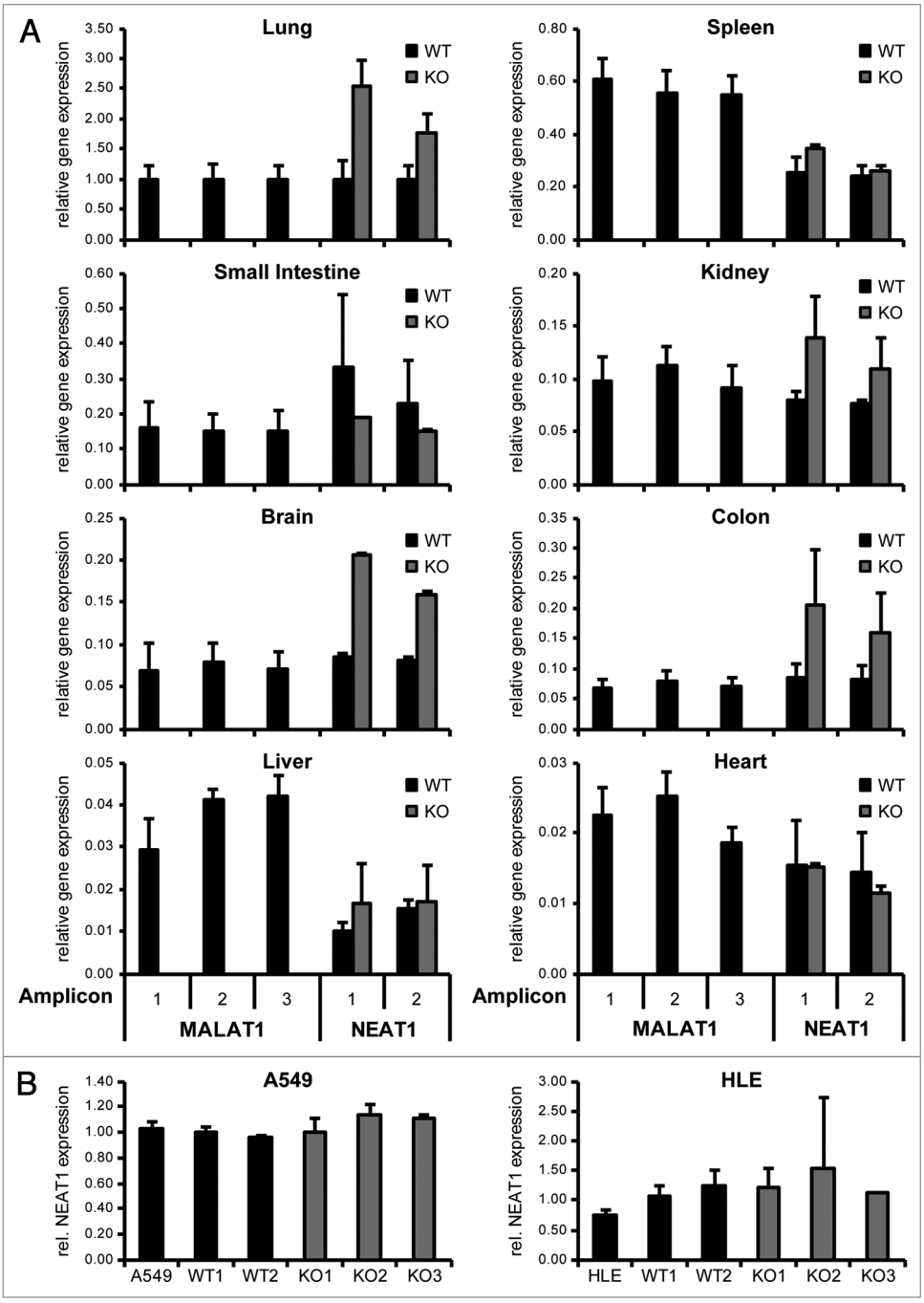

Figure 5. *Malat1* and *Neat1* expression. *Malat1* and *Neat1* expression were determined in eight different mouse tissues (A) and two human cancer cell lines (B) by qRT-PCR. (A) *Malat1* was quantified with three independent amplicons and *Neat1* was quantified using two independent amplicons in lung, spleen, small intestine, kidney, brain, colon, liver and heart of four wild-type (WT) and three *Malat1* knockout mice (KO). *Gapdh* served as reference gene and data was normalized to expression in normal lung which displayed the highest *Malat1* and *Neat1* expression. Depicted is the average expression +SEM (B) *NEAT1* was quantified in A549 and HLE cancer cell lines in the parental cell line, two wild-type clones (WT) and three *MALAT1* knockout clones (KO) each. *RN7SL1* served as reference gene, and data was normalized to expression in the wild-type cells. Depicted is the average expression +SEM.

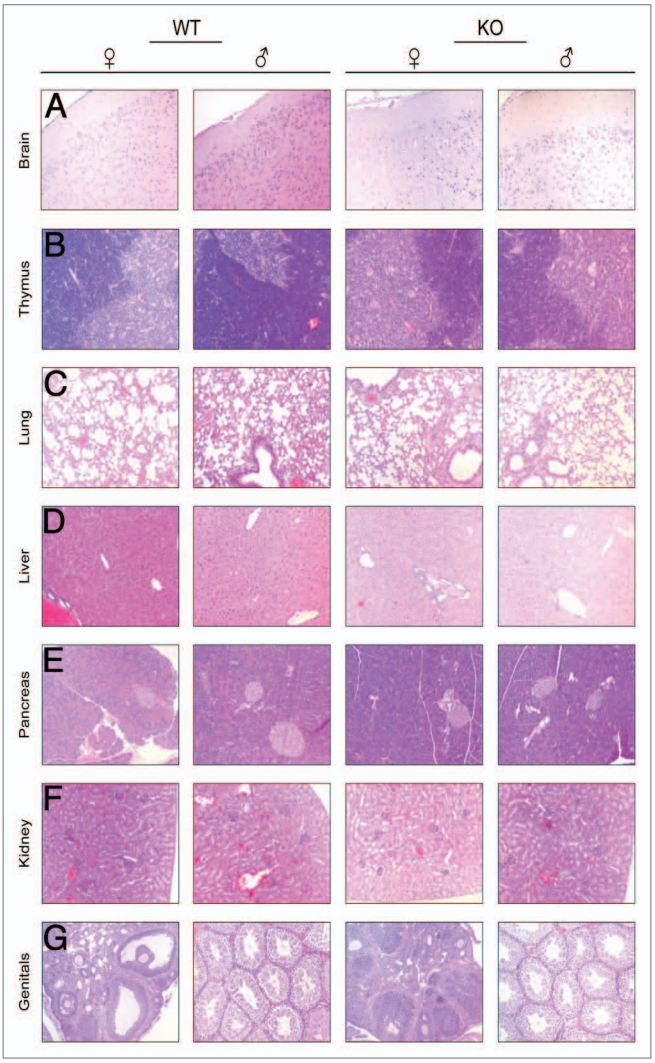

Figure 6. Depletion of *Malat1* does not alter organ histomorphology. H&E staining of brain (A), thymus (B), lung (C), liver (D), pancreas (E), kidney (F) and genitals (G) from wild-type *Malat1*$^{+/+}$ (left panel; ♀,♂) and knockout *Malat1*$^{-/-}$ (right panel; ♀,♂) mice. No histomorphogical differences were observed between wild-type and knockout mice in all tissues examined.

mice did not display any signs of developmental or histological abnormalities.

Discussion

The highly abundant, nuclear and evolutionarily conserved lncRNA *MALAT1* had been associated with many important cellular functions, linked to molecular mechanisms and was found to be deregulated in many physiological and pathological conditions.[11,13,21-33,35,38] Thus, we aimed to generate genetic knockout models to study its function and significance in vivo. Loss-of-function models were successfully established in human cancer cell lines as well as in a knockout mouse model. The zinc finger nuclease-mediated insertion of polyA signals into the *MALAT1* locus has been proven to be effective in gene silencing in lung cancer cells before.[41] Here, this methodology also effectively shuts down *MALAT1* expression more than 200-fold in human liver cancer cells. Hence, this knockout approach is more effective and more specific than standard RNA interference techniques[30,31] to deplete this highly abundant lncRNA. In addition, we have generated *Malat1* knockout mice using homologous recombination in ES cells to study the physiological function of *Malat1* in a whole mammalian organism.

Remarkably, we find *MALAT1* to be dispensable for cell viability, proliferation and development in the human and the mouse system, respectively. Given its many reported functional associations, its high expression, regulation and evolutionary conservation, this result is very surprising - in particular considering three previous findings: First, *MALAT1* knockdown via RNA interference suppressed proliferation in CaSki cervical cancer cells[22] unraveling a critical role for *MALAT1* in this cancer hallmark capability. Second, *MALAT1* had been found to govern the transcription of growth control genes.[11] Lastly, *MALAT1* had been associated with the trophoblast invasion and placenta function.[32] Despite all of the above mentioned evidence pointing to an important and and potentially essential function of *MALAT1*, our results clearly demonstrate that its quantitative loss in cancer cells does not affect proliferation and its knockout in mice does not affect viability or normal development.

These apparent discrepancies lead to the hypothesis that *MALAT1* could have cell type-specific functions, e.g., might be important for cervical cancer cell proliferation, but not for other cell types including A549 and HLE cells. Depending on further in-depth investigations, it might serve as a paradigm for a lncRNA that is ubiquitously expressed and highly conserved but nevertheless fulfills multiple different, non-essential and tissue-specific functions depending on the cellular environment or the availability of RNA-binding interaction partners.

Our findings also emphasize the need for clean and quantitative genetic loss-of-function models–as exemplified here in both a human as well as a murine system. RNA interference-based knockdown using siRNA or shRNA constructs undisputedly has its value in interrogating a gene for its function in vivo, but these approaches also need to be critically questioned for the efficiency and specificity of their knockdown, for possible off-target effects, and they need to be reproduced with a large number of siRNAs or shRNAs to validate a gene-specific effect. However, definitive answers on the question whether a gene is essential for metazoan development and viability or not can only be derived from knockout models.

While the *Malat1* knockout mouse does not display any detectable developmental or lethality phenotype, future studies will be essential to expose these mice to different stresses and environments. Such experiments will potentially reveal differences between wild-type and knockout animals that are due to the loss of *MALAT1* and further uncover its function in health and disease. Most interesting will be the studies on potential tumor phenotypes by crossing these mice to different cancer models since *MALAT1* has been discovered and most often linked to malignant diseases. The first description of *MALAT1* had identified it as a marker in lung cancer metastasis[21] and the

human and murine knockout models presented here now allow the in-depth analysis whether *MALAT1* might also represent an active player in the metastatic cascade despite not being an essential gene for life and development.

Materials and Methods

Cell culture. A549 lung adenocarcinoma cells were purchased from ATCC (CCL-185). HLE hepatocellular carcinoma cells were a kind gift of Dr. Britta Skawran (Hannover Medical School). Cells were cultivated at 37°C, 5% CO_2 in DMEM + 10% FBS, 0.2 mM Glutamine and antibiotics. A549 and HLE *MALAT1* KO cells were generated as previously published.[41]

RNA isolation and DNase I digest. RNA from cancer cell lines was isolated using the TRIzol reagent (Life Technologies) according to the manufacturer's recommendations. Samples were treated with DNase I (Roche) for 30 min at 37°C followed by a phenol:chloroform extraction and an ethanol precipitation at -80°C. For mouse tissue RNA isolation from snap frozen samples, the AllPrep RNA/DNA kit (Qiagen) was used according to the manufacturer's recommendations.

Reverse transcription and qRT-PCR. RNA (1–2 μg) was reverse transcribed with RevertAid™ reverse transcriptase (Thermo Scientific) according to the manufacturer's recommendations. Complete removal of genomic DNA was controlled in minus-RT samples in which the reverse transcriptase was replaced by water. For qRT-PCR, the ABI PowerSYBR Green PCR Master Mix was used, and the analysis was performed with an ABI StepOne Plus cycler (Life Technologies). Primer sequences can be found in **Table 1**.

Table 1. Primers used for qRT-PCR analysis

Gene	Forward	Reverse
human *MALAT1 5'end*	GAA TTG CGT CAT TTA AAG CCT AGT T	GTT TCA TCC TAC CAC TCC CAA TTA AT
human *MALAT1 3'End*	AAA GCA AGG TCT CCC CAC AAG	GGT CTG TGC TAG ATC AAA AGG CA
human *NEAT1*	CCA GTT TTC CGA GAA CCA AA	ATG CTG ATC TGC TGC GTA TG
murine *Malat1* Amplicon 1	TGA AAA AGG AAA TGA GGA GAA AAG	CTT CAC AAA ACC TCC CTT TAC AAT
murine *Malat1* Amplicon 2	TTC CAA AAA GAC CTG TAG AGC TG	AGG AAT TTT TAA GAG GCT GGA TG
murine *Malat1* Amplicon 3	TTT TCC CCT TGC CTG TAA TTT	CAC CCC AAC AAC TTC CTAC AA
murine *Neat1* Amplicon 1	GTG GGT TGA TGG GAA TAA CAG T	GCT CTT CCC CTT GTA GGA TTT T
murine *Neat1* Amplicon 2	AGA AGA TTG CGT AAG GTG TAG GAC	TTT CAG TTA AGA ATC CCT CTG ACC
human *RN7SL1*	ATC GGG TGT CCG CAC TAA GTT	CAG CAC GGG AGT TTT GAC CT
human *RPLP0*	GGC GAC CTG GAA GTC CAA CT	CCA TCA GCA CCA CAG CCT TC
murine *Gapdh*	TGG TGA AGC AGG CAT CTG AG	TGC TGT TGA AGT CGC AGG AG

All sequences are given in the 5'–3' orientation.

Proliferation assay. Cell proliferation was analyzed with the Cell Proliferation ELISA BrdU assay (Roche) according to the manufacturer's recommendations. Briefly, 5 x 10^3 were seeded into black 96-well plates with a clear bottom (Greiner Bio-One). After 48 h, the BrdU solution (10 μM f.c.) was added and the cells were incubated for 6 h. The chemiluminescence was measured with a luminometer (Fluoroskan Ascent FL; Thermo Scientific).

Cell cycle analysis. Cell cycle distribution of exponentially growing cells was analyzed according to standard protocols using Propidiumiodide (PI) staining for DNA content. Briefly, 3 x 10^5 cells were seeded 48 h prior to analysis in 10 cm dishes in normal growth medium. Cells were washed twice in phosphate buffered saline (PBS), scraped off the plates using a rubber policeman, fixed in ethanol, and RNA was digested with RNase A. Cell pellets were resuspended in PI staining solution (40 μg/mL f.c. PI in PBS). Cell cycle profiles were acquired using a BD FACS Calibur and analyzed using the Cell Quest Pro software (Becton Dickinson).

Fluorescence microscopy analysis of nuclear structures. Immunofluorescence, RNA staining via labeling of incorporated ethynyl uridine and staining of the DNA with 4',6-diamidin-2'-phenylindol-dihydrochlorid (DAPI) were conducted after para-Formaldheyde (PFA) fixation as described previously.[43] The antibodies used detected active RNA polymerase II (H5, GeneTex), lamin A (provided by Harald Herrmann-Lerdon, DKFZ), UBF (provided by Ingrid Grummt, DKFZ), SC35 (mouse α-SC35, Sigma-Aldrich), HP1α (Euromedex) and TRF2 (Calbiochem/Merck). For confocal fluorescence imaging, a Leica TCS SP5 confocal laser scanning microscope equipped with a HCX PL APO lambda blue 63x/1.4 NA oil immersion objective was used.

Establishment of an inducible *Malat1* knockout mouse model. The mouse *Malat1* gene locus was subcloned from the BAC clone RP24–290K10 (BACPAC Resources Center, Children's Hospital Oakland Research Institute; the library RP24 was generated from a single male C57Bl/6J mouse). For the construction of the *Malat1* knockout targeting vector, a previously published methodology and protocol was adjusted and used.[48] Briefly, short 500 bp homology arms (one 7 kb upstream of the *Malat1* transcription start (5'-arm) and one 1.9 kb downstream of the *Malat1* transcript (3'-arm) were amplified by PCR with BAC clone RP24_290K10 as template DNA and inserted via restriction/ligation into the *pKoII* vector backbone. The BAC clone was electroporated into the recombination-competent *E. coli* strain SW106.[48] The bacteria are available from the NCI Frederick (https://notendur.hi.is/bmo/Recombineering%20Website.htm). The bacteria were transformed with the XhoI/Sal1 linearized *pKoII* vector. In the bacteria, the *Malat1* locus with the 7 kb upstream and the 1.9 kb downstream areas was recombined into the *pKoII* vector backbone. Genomic sequences directly downstream of the murine *Malat1* gene were amplified by PCR and inserted in front and behind the *FRT-Neo-FRT-loxP* cassette

in the *pl45.1* vector. The *5'-arm-FRT-Neo-FRT-loxP-3'-arm* fragment was excised by KpnI, SacII and ApaL1 and recombined downstream of the *Malat1* gene into the *pKoII* vector. Restriction by SpeI and ligation of the loxP double-stranded oligonucleotide 5' of the *Malat1* transcription start in the *pKoII* vector completed the *Malat1* knockout targeting construct which was verified by sequencing.

The (*5'-arm-loxP-Malat1-FRT-Neo-FRT-loxP-3'-arm*) targeting vector was linearized by NotI and electroporated into the embryonic stem cell (ES) line V6.5 (SV129 x Bl6 F1 hybrid). G418-resistant ES clones were screened for correct homologous recombination at the *Malat1* locus via colony PCR and Southern Blot analysis. For the colony PCR reaction, the following primer sequences were used: neo forward 5'-TTC TGA GGG GAT CAA TTC TCT AGA GCT CGC-3'(located in the neo gene sequence) and wt reverse 5'-CTC ACC TGG AAC CCT CTA TGT AGA ACA GC-3' (located immediately downstream and outside of the targeting vector within the wildtype sequence). In case of correct homologous recombination of the targeting vector, a 2420 bp PCR fragment was amplified (**Fig. 4B**). For Southern Blot analysis, the external probe 2 was generated by PCR amplification of genomic sequence using the primers fwd_probe2 (5'-AGC TCT GAG TGC CTG TTT CTG-3') and rev_probe2 (5'-ATG CTC TCT CCC ACA TGA CC-3'). The resulting 680 bp fragment was subcloned and used for conventional Southern Blotting using established protocols. Genomic DNA isolated from ES cell clones was digested with BamHI and XhoI; hybridization with the [^{32}P]-labeled probe 2 produced a 10.6 kb BamHI/BamHI wildtype signal and a 4.1 kb XhoI/BamHI signal in case of correct targeting of the *Malat1* locus (**Fig. 4C**).

Positive ES cell clones were injected into blastocysts derived from C57Bl/6J mice (Charles River), and chimeric animals were set up for breeding with wildtype C57Bl/6J mice to identify animals transmitting the correctly targeted *Malat1* locus via the germ line. The heterozygous *Malat1*loxP,FRTNeo/+ mice generated from the ES cell clones were crossed with a transgenic CMV-Cre deleter line (in a C57Bl/6J genetic background) to remove the PGK-Neo selection cassette and the complete *Malat1* gene, which was confirmed by PCR (**Fig. 4D** and below). As a result, nucleotides 5795370–5802920 from mouse chromosome 19qA (Assembly NCBI37/mm9) consisting of the complete 6982 nt *Malat1* transcript sequence plus 251 nt upstream of the *Malat1* transcription start site and 322 nt downstream of the *Malat1* transcript end were removed.

Genotyping of constitutive *Malat1* knockout mice. A three-primer-PCR strategy was used for genotyping the constitutive *Malat1* knockout mice. Primer 1 (5'-CAC TCT GGG AAT GTT TTT GG-3'), Primer 2 (5'-CAG GAA AAC GCA AAA GGT GT-3') and Primer 3 (5'-TGT CGA AAA GAG GTG GTG TG-3') as indicated in **Figure 4D** (10 μM each) produced a 120 bp fragment for the wild-type allele and a 204 bp fragment for the *Malat1*-deleted locus. PCR conditions were as follows: 4 min 95°C, followed by 30 cycles of 30 sec 95°C, 30 sec 56°C, 30 sec 72°C, and a final elongation for 10 min at 72°C.

Histomorphological analysis. Mice were sacrificed at the age of 6 weeks. Tissues were resected, fixed in 4% formaldehyde and embedded in paraffin for subsequent staining. Five micrometer sections were cut and stained with hematoxylin and eosin (H&E) according to standard procedures. Histopathologic review of the H&E slides for histopathologic abnormalities was performed using an Olympus BX51 microscope and pictures were taken using a ProgRes® CMOS camera (Jenoptik). All animal experiments were done in accordance with the Guide for the Care and Use of Laboratory Animals published by the US National Institutes of Health (NIH Publication No. 85–23, revised 1996) and according to the regulations issued by the Committee for Animal Rights Protection of the States of Hessen (Regierungspräsidium Darmstadt).

Statistical analysis. Statistical analyses were performed using Excel 2007. Significance was assessed using T-Tests after determination of the variance equality using an F-Test.

Disclosure of Potential Conflicts of Interest

No potential conflicts of interest were disclosed.

Acknowledgments

We thank Dr. Kai Breuhahn for expert help with mouse preparation. We are grateful to Susanne Kreuzer, Sonja Krüger (both MPI Bad Nauheim) and Susanne Bösser (Georg-Speyer-Haus) for excellent technical assistance and ES cell culture. Research in the Diederichs lab is supported by the German Research Foundation (DFG Transregio TRR77, TP B03), the Marie Curie Program of the European Commission, the Helmholtz Society (VH-NG-504), the Virtual Helmholtz Institute for Resistance in Leukemia, the German Cancer Research Center (DKFZ), and the Institute of Pathology, University of Heidelberg. T.G. is supported by a DKFZ PhD Fellowship. This work was supported by the Graduiertenkolleg 1172 (to M. E. and M. Z.) and institutional funds of the Georg-Speyer-Haus (M.Z.). The Georg-Speyer-Haus is funded jointly by the German Federal Ministry of Health (BMG) and the Ministry of Higher Education, Research and the Arts of the state of Hessen (HMWK). M.Z. is supported by the LOEWE Center for Cell and Gene Therapy Frankfurt [HMWK III L 4-518/17.004 (2010)] and the LOEWE initiative Oncogenic Signaling Frankfurt [HMWK III L 4-518/55.004 (2009)].

Note added in proof

While our manuscript was in press, two novel publications came to our attention describing similar phenotypes for the Malat1 knockout mice from the laboratories of David Spector[49] and Shinichi Nakagawa and Kannanganattu Prasanth.[50]

References

1. Birney E, Stamatoyannopoulos JA, Dutta A, Guigó R, Gingeras TR, Margulies EH, et al.; ENCODE Project Consortium; NISC Comparative Sequencing Program; Baylor College of Medicine Human Genome Sequencing Center; Washington University Genome Sequencing Center; Broad Institute; Children's Hospital Oakland Research Institute. Identification and analysis of functional elements in 1% of the human genome by the ENCODE pilot project. Nature 2007; 447:799-816; PMID:17571346; http://dx.doi.org/10.1038/nature05874.
2. Cabili MN, Trapnell C, Goff L, Koziol M, Tazon-Vega B, Regev A, et al. Integrative annotation of human large intergenic noncoding RNAs reveals global properties and specific subclasses. Genes Dev 2011; 25:1915-27; PMID:21890647; http://dx.doi.org/10.1101/gad.17446611.
3. Carninci P, Kasukawa T, Katayama S, Gough J, Frith MC, Maeda N, et al.; FANTOM Consortium; RIKEN Genome Exploration Research Group and Genome Science Group (Genome Network Project Core Group). The transcriptional landscape of the mammalian genome. Science 2005; 309:1559-63; PMID:16141072; http://dx.doi.org/10.1126/science.1112014.
4. Clark MB, Amaral PP, Schlesinger FJ, Dinger ME, Taft RJ, Rinn JL, et al. The reality of pervasive transcription. PLoS Biol 2011; 9:e1000625, discussion e1001102; PMID:21765801; http://dx.doi.org/10.1371/journal.pbio.1000625.
5. Winter J, Jung S, Keller S, Gregory RI, Diederichs S. Many roads to maturity: microRNA biogenesis pathways and their regulation. Nat Cell Biol 2009; 11:228-34; PMID:19255566; http://dx.doi.org/10.1038/ncb0309-228.
6. Nagano T, Fraser P. No-nonsense functions for long noncoding RNAs. Cell 2011; 145:178-81; PMID:21496640; http://dx.doi.org/10.1016/j.cell.2011.03.014.
7. Wang KC, Chang HY. Molecular mechanisms of long noncoding RNAs. Mol Cell 2011; 43:904-14; PMID:21925379; http://dx.doi.org/10.1016/j.molcel.2011.08.018.
8. Wilusz JE, Sunwoo H, Spector DL. Long noncoding RNAs: functional surprises from the RNA world. Genes Dev 2009; 23:1494-504; PMID:19571179; http://dx.doi.org/10.1101/gad.1800909.
9. Rinn JL, Kertesz M, Wang JK, Squazzo SL, Xu X, Brugmann SA, et al. Functional demarcation of active and silent chromatin domains in human HOX loci by noncoding RNAs. Cell 2007; 129:1311-23; PMID:17604720; http://dx.doi.org/10.1016/j.cell.2007.05.022.
10. Tsai MC, Manor O, Wan Y, Mosammaparast N, Wang JK, Lan F, et al. Long noncoding RNA as modular scaffold of histone modification complexes. Science 2010; 329:689-93; PMID:20616235; http://dx.doi.org/10.1126/science.1192002.
11. Yang L, Lin C, Liu W, Zhang J, Ohgi KA, Grinstein JD, et al. ncRNA- and Pc2 methylation-dependent gene relocation between nuclear structures mediates gene activation programs. Cell 2011; 147:773-88; PMID:22078878; http://dx.doi.org/10.1016/j.cell.2011.08.054.
12. Ankö ML, Neugebauer KM. Long noncoding RNAs add another layer to pre-mRNA splicing regulation. Mol Cell 2010; 39:833-4; PMID:20864030; http://dx.doi.org/10.1016/j.molcel.2010.09.003.
13. Tripathi V, Ellis JD, Shen Z, Song DY, Pan Q, Watt AT, et al. The nuclear-retained noncoding RNA MALAT1 regulates alternative splicing by modulating SR splicing factor phosphorylation. Mol Cell 2010; 39:925-38; PMID:20797886; http://dx.doi.org/10.1016/j.molcel.2010.08.011.
14. Zong X, Tripathi V, Prasanth KV. RNA splicing control: yet another gene regulatory role for long nuclear noncoding RNAs. RNA Biol 2011; 8:968-77; PMID:21941126; http://dx.doi.org/10.4161/rna.8.6.17606.
15. Payer B, Lee JT. X chromosome dosage compensation: how mammals keep the balance. Annu Rev Genet 2008; 42:733-72; PMID:18729722; http://dx.doi.org/10.1146/annurev.genet.42.110807.091711.
16. Tian D, Sun S, Lee JT. The long noncoding RNA, Jpx, is a molecular switch for X chromosome inactivation. Cell 2010; 143:390-403; PMID:21029862; http://dx.doi.org/10.1016/j.cell.2010.09.049.
17. Gutschner T, Diederichs S. The Hallmarks of Cancer: A long non-coding RNA point of view. RNA Biol 2012; 9: In press; PMID:22664915; http://dx.doi.org/10.4161/rna.20481.
18. Spizzo R, Almeida MI, Colombatti A, Calin GA. Long non-coding RNAs and cancer: a new frontier of translational research? Oncogene 2012; PMID:22266873; http://dx.doi.org/10.1038/onc.2011.621.
19. Tsai MC, Spitale RC, Chang HY. Long intergenic noncoding RNAs: new links in cancer progression. Cancer Res 2011; 71:3-7; PMID:21199792; http://dx.doi.org/10.1158/0008-5472.CAN-10-2483.
20. Prensner JR, Chinnaiyan AM. The emergence of lncRNAs in cancer biology. Cancer Discov 2011; 1:391-407; PMID:22096659; http://dx.doi.org/10.1158/2159-8290.CD-11-0209.
21. Ji P, Diederichs S, Wang W, Böing S, Metzger R, Schneider PM, et al. MALAT-1, a novel noncoding RNA, and thymosin beta4 predict metastasis and survival in early-stage non-small cell lung cancer. Oncogene 2003; 22:8031-41; PMID:12970751; http://dx.doi.org/10.1038/sj.onc.1206928.
22. Guo F, Li Y, Liu Y, Wang J, Li Y, Li G. Inhibition of metastasis-associated lung adenocarcinoma transcript 1 in CaSki human cervical cancer cells suppresses cell proliferation and invasion. Acta Biochim Biophys Sin (Shanghai) 2010; 42:224-9; PMID:20213048; http://dx.doi.org/10.1093/abbs/gmq008.
23. Lin R, Maeda S, Liu C, Karin M, Edgington TS. A large noncoding RNA is a marker for murine hepatocellular carcinomas and a spectrum of human carcinomas. Oncogene 2007; 26:851-8; PMID:16878148; http://dx.doi.org/10.1038/sj.onc.1209846.
24. Yamada K, Kano J, Tsunoda H, Yoshikawa H, Okubo C, Ishiyama T, et al. Phenotypic characterization of endometrial stromal sarcoma of the uterus. Cancer Sci 2006; 97:106-12; PMID:16441420; http://dx.doi.org/10.1111/j.1349-7006.2006.00147.x.
25. Kong SL, Chui P, Lim B, Salto-Tellez M. Elucidating the molecular physiopathology of acute respiratory distress syndrome in severe acute respiratory syndrome patients. Virus Res 2009; 145:260-9; PMID:19635508; http://dx.doi.org/10.1016/j.virusres.2009.07.014.
26. Sun Y, Wu J, Wu SH, Thakur A, Bollig A, Huang Y, et al. Expression profile of microRNAs in c-Myc induced mouse mammary tumors. Breast Cancer Res Treat 2009; 118:185-96; PMID:18777135; http://dx.doi.org/10.1007/s10549-008-0171-6.
27. Xu C, Yang M, Tian J, Wang X, Li Z. MALAT-1: a long non-coding RNA and its important 3' end functional motif in colorectal cancer metastasis. Int J Oncol 2011; 39:169-75; PMID:21503572.
28. Fellenberg J, Bernd L, Delling G, Witte D, Zahlten-Hinguranage A. Prognostic significance of drug-regulated genes in high-grade osteosarcoma. Mod Pathol 2007; 20:1085-94; PMID:17660802; http://dx.doi.org/10.1038/modpathol.3800937.
29. Kryger R, Fan L, Wilce PA, Jaquet V. MALAT-1, a non protein-coding RNA is upregulated in the cerebellum, hippocampus and brain stem of human alcoholics. Alcohol 2012; PMID:22560368; http://dx.doi.org/10.1016/j.alcohol.2012.04.002.
30. Schmidt LH, Spieker T, Koschmieder S, Humberg J, Jungen D, Bulk E, et al. The long noncoding MALAT-1 RNA indicates a poor prognosis in non-small cell lung cancer and induces migration and tumor growth. J Thorac Oncol 2011; 6:1984-92; PMID:22088988; http://dx.doi.org/10.1097/JTO.0b013e3182307eac.
31. Tano K, Mizuno R, Okada T, Rakwal R, Shibato J, Masuo Y, et al. MALAT-1 enhances cell motility of lung adenocarcinoma cells by influencing the expression of motility-related genes. FEBS Lett 2010; 584:4575-80; PMID:20937273; http://dx.doi.org/10.1016/j.febslet.2010.10.008.
32. Tseng JJ, Hsieh YT, Hsu SL, Chou MM. Metastasis associated lung adenocarcinoma transcript 1 is up-regulated in placenta previa increta/percreta and strongly associated with trophoblast-like cell invasion in vitro. Mol Hum Reprod 2009; 15:725-31; PMID:19690017; http://dx.doi.org/10.1093/molehr/gap071.
33. Bernard D, Prasanth KV, Tripathi V, Colasse S, Nakamura T, Xuan Z, et al. A long nuclear-retained non-coding RNA regulates synaptogenesis by modulating gene expression. EMBO J 2010; 29:3082-93; PMID:20729808; http://dx.doi.org/10.1038/emboj.2010.199.
34. Lin R, Roychowdhury-Saha M, Black C, Watt AT, Marcusson EG, Freier SM, et al. Control of RNA processing by a large non-coding RNA over-expressed in carcinomas. FEBS Lett 2011; 585:671-6; PMID:21266177; http://dx.doi.org/10.1016/j.febslet.2011.01.030.
35. Hutchinson JN, Ensminger AW, Clemson CM, Lynch CR, Lawrence JB, Chess A. A screen for nuclear transcripts identifies two linked noncoding RNAs associated with SC35 splicing domains. BMC Genomics 2007; 8:39; PMID:17270048; http://dx.doi.org/10.1186/1471-2164-8-39.
36. Hafner M, Landthaler M, Burger L, Khorshid M, Hausser J, Berninger P, et al. Transcriptome-wide identification of RNA-binding protein and microRNA target sites by PAR-CLIP. Cell 2010; 141:129-41; PMID:20371350; http://dx.doi.org/10.1016/j.cell.2010.03.009.
37. Lebedeva S, Jens M, Theil K, Schwanhäusser B, Selbach M, Landthaler M, et al. Transcriptome-wide analysis of regulatory interactions of the RNA-binding protein HuR. Mol Cell 2011; 43:340-52; PMID:21723171; http://dx.doi.org/10.1016/j.molcel.2011.06.008.
38. Wilusz JE, Freier SM, Spector DL. 3' end processing of a long nuclear-retained noncoding RNA yields a tRNA-like cytoplasmic RNA. Cell 2008; 135:919-32; PMID:19041754; http://dx.doi.org/10.1016/j.cell.2008.10.012.
39. Clemson CM, Hutchinson JN, Sara SA, Ensminger AW, Fox AH, Chess A, et al. An architectural role for a nuclear noncoding RNA: NEAT1 RNA is essential for the structure of paraspeckles. Mol Cell 2009; 33:717-26; PMID:19217333; http://dx.doi.org/10.1016/j.molcel.2009.01.026.
40. Nakagawa S, Naganuma T, Shioi G, Hirose T. Paraspeckles are subpopulation-specific nuclear bodies that are not essential in mice. J Cell Biol 2011; 193:31-9; PMID:21444682; http://dx.doi.org/10.1083/jcb.201011110.
41. Gutschner T, Baas M, Diederichs S. Noncoding RNA gene silencing through genomic integration of RNA destabilizing elements using zinc finger nucleases. Genome Res 2011; 21:1944-54; PMID:21844124; http://dx.doi.org/10.1101/gr.122358.111.
42. Caudron-Herger M, Rippe K. Nuclear architecture by RNA. Curr Opin Genet Dev 2012; 22:179-87; PMID:22281031; http://dx.doi.org/10.1016/j.gde.2011.12.005.
43. Caudron-Herger M, Müller-Ott K, Mallm JP, Marth C, Schmidt U, Fejes-Tóth K, et al. Coding RNAs with a non-coding function: maintenance of open chromatin structure. Nucleus 2011; 2:410-24; PMID:21983088; http://dx.doi.org/10.4161/nucl.2.5.17736.

44. Papantonis A, Cook PR. Genome architecture and the role of transcription. Curr Opin Cell Biol 2010; 22:271-6; PMID:20356724; http://dx.doi.org/10.1016/j.ceb.2010.03.004.
45. Mao YS, Zhang B, Spector DL. Biogenesis and function of nuclear bodies. Trends Genet 2011; 27:295-306; PMID:21680045; http://dx.doi.org/10.1016/j.tig.2011.05.006.
46. Shevtsov SP, Dundr M. Nucleation of nuclear bodies by RNA. Nat Cell Biol 2011; 13:167-73; PMID:21240286; http://dx.doi.org/10.1038/ncb2157.
47. Schwenk F, Baron U, Rajewsky K. A cre-transgenic mouse strain for the ubiquitous deletion of loxP-flanked gene segments including deletion in germ cells. Nucleic Acids Res 1995; 23:5080-1; PMID:8559668; http://dx.doi.org/10.1093/nar/23.24.5080.
48. Liu P, Jenkins NA, Copeland NG. A highly efficient recombineering-based method for generating conditional knockout mutations. Genome Res 2003; 13:476-84; PMID:12618378; http://dx.doi.org/10.1101/gr.749203.
49. Zhang B, Arun G, Mao YS, Lazar Z, Hung G, Bhattacharjee G, et al. The lncRNA Malat1 is dispensable for mouse development but its transcription plays a cis-regulatory role in the adult. Cell Rep 2012; 1: In press.
50. Nakagawa S, Ip JY, Shioi G, Hirose T, Prasanth KV. Malat1 is not essential in mouse but controls efficient formation of paraspeckles in particular tissues. RNA 2012; 18: In press.